Arab J Geosci
DOI 10.1007/s12517-015-1870-z

ORIGINAL PAPER

Studying the spatial distribution of maximum monthly rainfall in selected regions of Saudi Arabia using geographic information systems

Bashar Bashir · Hesham Fouli

Received: 29 October 2014 / Accepted: 26 February 2015

Abstract This paper presents the results of studying the spatial distribution of the maximum monthly rainfall within the Kingdom of Saudi Arabia (KSA) using geographic information systems (GIS). Isohyetal maps were constructed based on long historical rainfall depth data (1963–2013) of 255 rain gauges, after processing the data using different interpolation methods and their conversion to grid raster. Six interpolation methods were used: (a) kriging, (b) spline, (c) natural neighbor, (d) inverse distance weighting (IDW), (e) modified Shepard, and (f) triangulation with linear interpolation (TIN). Estimations of the rainfall at the rain gauges were compared to the observed measurements as controls and the method that resulted in minimum residuals and minimum standard deviation; in this case, the IDW was selected for the study. The percentage of residuals within ±2.0 mm were found to be 98 % for IDW, modified Shepard, and TIN, 97 % for natural neighbor, 90 % for spline, and 32 % for kriging. While identifying potential water harvesting sites depends on many factors, such as watershed area, topography, morphology, and rainfall, the results of this study can be used for the primary selection of water harvesting sites based on rainfall being the most important factor.

B. Bashir · H. Fouli (✉)
Chair of Prince Sultan Bin Abdulaziz International Prize for Water, Prince Sultan Institute for Environmental, Water and Desert Research, King Saud University, P.O. Box 2454, Riyadh 11451, Saudi Arabia
e-mail: hfouli@ksu.edu.sa

B. Bashir
e-mail: bbashir@ksu.edu.sa

B. Bashir · H. Fouli
Department of Civil Engineering, King Saud University, P.O. Box 800, Riyadh 11421, Saudi Arabia

Keywords Rainwater harvesting · GIS · Arid regions · Grid raster · Interpolation methods

Introduction

Rainwater harvesting is a technology used to collect, convey, and store rain water for later use by communities. It covers a wide spectrum of techniques that ranges from roof-based systems in houses to land-based or watershed systems, which include dams and reservoirs. Roof-based systems are applicable locally in cities and towns, where direct runoff from roofs of buildings is collected through gutters and pipes into in-house tanks for storage and use. Land-based rainwater harvesting, on the other hand, occurs when runoff from land surfaces (catchment areas or watersheds) is collected in furrow dikes, ponds, tanks, and reservoirs and is the focus of this paper. Gould and Nissen-Petersen (1999) categorized rainwater harvesting according to the type of catchment surface used and the scale of activity. Water harvested from rainfall and surface runoff, unlike groundwater, has the advantage that it usually has better quality and therefore is easier to use by humans and animals and for irrigation with inexpensive and simple treatment techniques. Rainwater harvesting and storage also relieves the pressure on sewers and environment by mitigating floods and soil erosion, in addition to replenishing groundwater.

Water harvesting can be defined as the process of concentrating rainfall as runoff from a larger catchment area to be used in a smaller target area. This process may occur naturally or artificially. The collected runoff water is either directly applied to an adjacent agricultural field (or plot) or stored in some type of on-farm storage facility for domestic use and as supplemental irrigation of crops. All rainfall harvesting systems have three components: a collection area, a conveyance system, and a storage area. The use of rainwater

Published online: 24 April 2015

collection systems is known to have existed 4000 years ago in the semiarid and arid regions of the Negev Desert, Palestine, which receives less than 150 mm of annual rainfall. Water harvesting is an ancient art that was practiced in the past in many parts of the World including North America, Middle East, North Africa, China, and India.

Several rainwater and runoff harvesting studies utilized GIS techniques for selecting potential water harvesting locations. For example, de Winnaar et al. (2007) used GIS to identify potential runoff harvesting sites at the Potshini catchment, a small sub-catchment in the Thukela River basin, South Africa. Al-Adamat (2008) used GIS for siting water harvesting ponds in the Basalt Aquifer, Jordan. Bakir and Xingnan (2008) used GIS and remote sensing application for rainwater harvesting in the Syrian Desert. Bargaoui and Chebbi (2009) compared the accuracy of both 2-D classical procedure and 3-D estimation of variogram structure for spatial-temporal rainfall analysis using cross-validation scheme. They used two recorded extreme events in north and northeast Tunisia in 1973 and 1986. Their results showed that the 3-D Kriging leads to much smaller prediction errors than the 2-D Kriging.Al-Adamat et al. (2010) used both the Weighted Linear Combination and the Boolean techniques within GIS environment to select suitable areas in Northern Jordan for establishing water harvesting ponds. Hadadin et al. (2012) used GIS and digital elevation model to identify potential water harvesting sites in the north-east Badia of Jordan. Chen and Liu (2012) used inverse distance weighting (IDW) to estimate the spatial rainfall distribution in the middle of Taiwan.

Many studies were made to quantify the hydrological characteristics and flood probability in Saudi Arabia, particularly the rainier southwest and west regions. Some of these studies adopted extreme value analyses methods, such as Gumble and Log Pearson type III (Al-Turbak and Quraishi 1986; AlHassoun 2011; Elsebaie 2011; Subyani 2011), while others used Fisher-Cornish model (Al-Zahrani 1989; Abouammoh 1991). Wheater et al. (1991a) formulated a stochastic multivariate spatial-temporal model for rainfall distribution within five basins in Southwest Saudi Arabia based on hourly rain data. Wheater et al. (1991b) evaluated long-term performance of rain gauges using regional analysis. Al-Zahrani and Hussain (1998) applied a hydrological network design method, on the basis of Shannon's information measure, and showed that the existing 70 rainfall stations within certain hydrological area on the Red Sea coast then could be reduced to 45 stations including new ones. Alazba (2004) developed contour maps for hydrologic and climatic parameters in Kingdom of Saudi Arabia (KSA). More recently, Amin et al. (2013) suggested a soft-path water management strategy to avoid short-term flooding problems in urban areas using rooftop water harvesting and management. Mahmoud and Alazba (2014) constructed a suitability map for potential rainwater harvesting sites in some arid regions of KSA using GIS, remote sensing (RS) data, and field survey. Mahmoud et al. (2014) used the same procedure to identify ground water recharge in Jazan Region of KSA.

Due to the scarcity of fresh water in KSA, it is crucial that rain water is utilized to the utmost potential. Being in arid region, KSA receives approximate mean annual precipitation of only 100 mm, most of which occurs in the west and southwest regions (Climate Atlas of Saudi Arabia 1988). While the data of the Climate Atlas of Saudi Arabia is fairly old, the mean annual precipitation over KSA has been calculated in this study using data up to 2013 and was found to be approximately 102 mm. The fast development taking place in KSA at present poses pressure on making more water available for users. Many dams have been constructed for the purpose of rainwater harvesting and groundwater recharge. King Fahd Project for Rainwater and Floodwater Harvesting and Storage was carried out in 2004 by Prince Sultan Institute for Environmental, Water, and Desert Research (http://www.unoosa.org/pdf/pres/stsc2010/tech-50.pdf). The project aimed at increasing water resources, especially for rural settings, and mitigating flash floods' hazards. The central zone of KSA including the provinces of Riyadh, Qassim, Hail, and Jouf, however, faces the highest challenges being far from the coasts and with fewer rain (see Fig. 1). For these reasons, this central zone has been selected as a study area.

The objective of this research is to study the spatial rainfall distribution of the maximum monthly rainfall by applying different interpolation methods while using GIS. While the study focuses on only the central zone of KSA, other provinces may adopt the same methodology to locate areas of maximum rainfall. While identifying potential water harvesting sites depends on many factors, such as watershed area, topography, morphology, and rainfall, the results of this study can be used for the primary selection of water harvesting sites based on rainfall being the most important factor.

Background on the interpolation methods

Six interpolation methods have been selected in the present study; they are: kriging, spline, natural neighbor, inverse distance weighting (IDW), modified Shepard, and triangulation with linear interpolation (TIN). This section provides brief description on each of these methods.

Kriging interpolation method

Kriging uses the covariance structure of the field measurements at specific points, to estimate interpolated values. The resulting interpolated field is optimal in the sense of minimizing the variance among all possible linear,

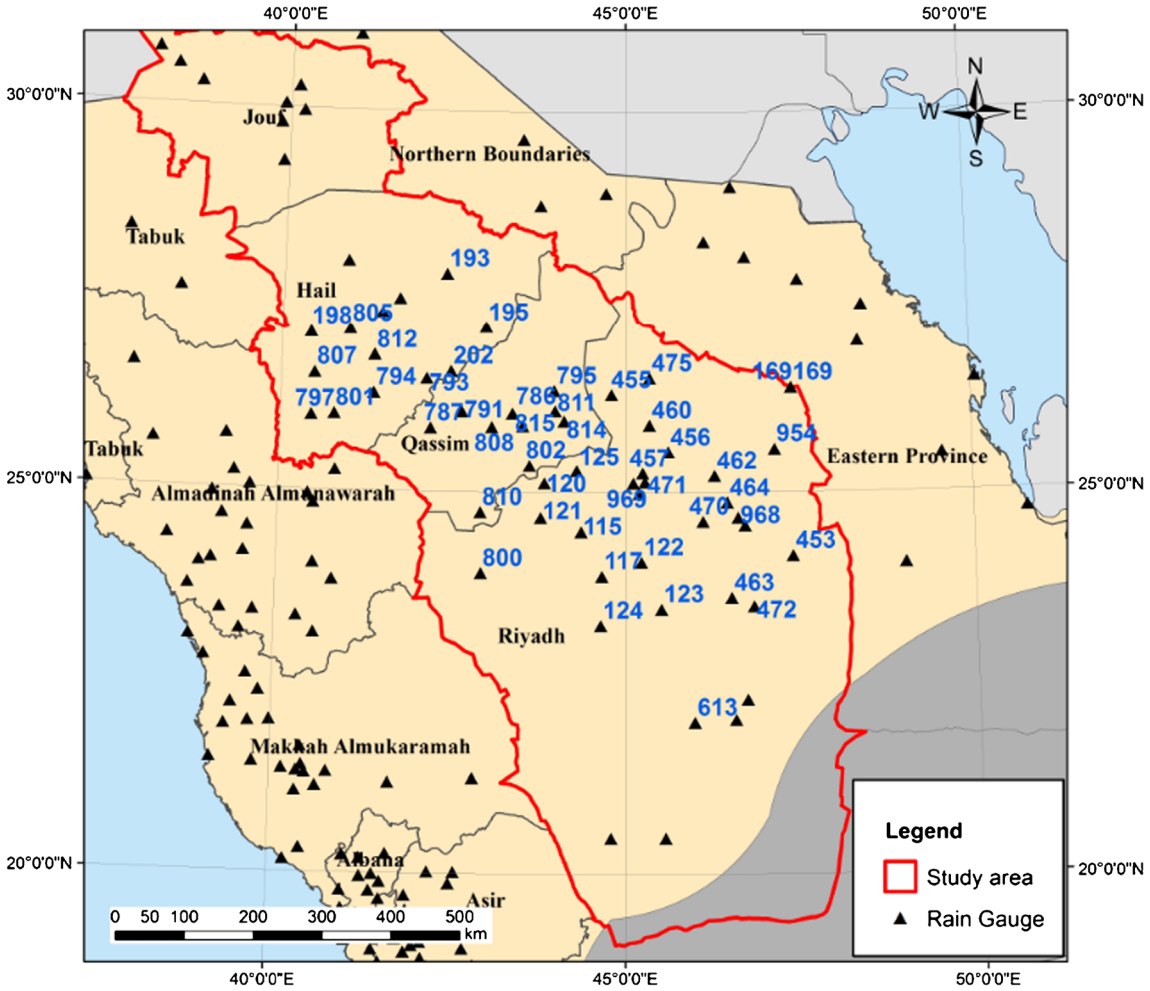

Fig. 1 Map of Saudi Arabia showing the locations of rain gauges and the study area with the administrative borders of the provinces

unbiased estimates. Kriging is a two-step process: (a) the fitting of a semivariogram model function (of distance) followed by (b) the solution of a set of matrix equations. An empirical semivariogram function (γ) is typically given by

$$\gamma(distance,\ h) = 0.5 * average((value\ i - value\ j))^2\Big) \quad (1)$$

where γ is computed for all pairs of locations separated by distance (h) and the values on the right side of Eq. 1 are of the rainfall depths at each pair (i, j). The semivariogram function basically depicts the spatial autocorrelation of the measured sample points.

Spline interpolation method

The spline mathematical functions are akin to the flexible ruler that was historically used to produce a smooth curve when joining a set of points. Spline functions can produce estimates that are above and below the measured minimum and maximum values. This is not always desired, as maxima and minima values are often produced where they do not occur in nature.

Natural neighbor interpolation method

The algorithm used by the natural neighbor interpolation method finds the closest subset of input samples to a query point and applies weights to them based on proportionate areas to interpolate a value (Sibson 1981). It is also known as Sibson or "area-stealing" interpolation. Its basic properties are that it is local, i.e., uses only a subset of samples that surrounds a query point, and interpolated heights are guaranteed to be within the range of the samples used. It does not infer trends and will not produce peaks, pits, ridges, or valleys that are not already represented by the input samples. The surface passes through the input samples and is smooth everywhere except at locations of the input samples.

IDW interpolation method

In this method, weights are calculated depending on the distances between the location where an estimate is required and the location where the rainfall is measured. Because moving average methods such as inverse distance weighted are by definition smoothing techniques, the maximum and minimum values can only occur at the measured points. This technique will therefore never produce a value that is higher than the maximum value in the observed data set. The fact that daily rainfall amounts are often confined to a small area causes another problem when using this type of interpolation, as rainfall amounts are generated for areas where no rain fell. These amounts do, however, decrease with distance, but there is not a sufficient spatial density of rain gauges to explain this (Lynch 2014).

Modified Shepard's method

The modified Shepard's method uses an inverse distance-weighted least squares method. As such, modified Shepard's method is similar to the inverse distance to a power interpolator, but the use of local least squares eliminates or reduces the "bull's-eye" appearance of the generated contours. Modified Shepard's method can be either an exact or a smoothing interpolator. The surfer algorithm implements Franke and Nielson's (1980) modified quadratic Shepard's method with a full sector search as described in Renka (1988).

The triangulation with linear interpolation method

The triangulation with linear interpolation method (TIN) in SURFER uses the optimal Delaunay triangulation algorithm. This algorithm creates triangles by drawing lines between data points. The original points are connected in such a way that no triangle edges are intersected by other triangles. The result is a patchwork of triangular faces over the extent of the grid. This method is an exact interpolator. Each triangle defines a plane over the grid nodes lying within the triangle, with the tilt and elevation of the triangle determined by the three original data points defining the triangle. All grid nodes within a given triangle are defined by the triangular surface. Because the original data are used to define the triangles, the data are honored very closely. TIN works best when your data are evenly distributed over the grid area. Data sets containing sparse areas result in distinct triangular facets on the map (Yang et al. 2004).

Methodology

Data collection and analyses

Rainfall data of various rain gauges that belong to the Ministry of Water and Electricity (MOWE) in KSA were used in the analyses. These rain gauges are distributed across KSA (see Fig. 1). A Delphi 7 computer code was developed and used to read and manipulate the data files of all rain gauges, particularly the mean annual, mean monthly, and maximum monthly records in each month for the period 1963–2013. The code extracts the rainfall data of each gauge, its coordinates, and the province where it exists. A climate normal is defined by convention as the mean of climatological variable over a 30-year period (WMO 1989). To comply with this definition, all rain gauges that have less than 30 years of rainfall depth continuous records were not considered in this study. A total of 255 rain gauges were considered in this study as listed in Table 1, which also presents the corresponding average data record length in years in each province.

Studying the spatial distribution of the rain gauge locations

The spatial distribution of the rain gauge locations has been studied using the Average Nearest Neighbor (ANN) tool of the Spatial Statistics toolbox of ArcGIS 10.0. ANN is calculated according to the following equation:

$$ANN = \frac{\overline{D}o}{\overline{D}_E} \tag{2}$$

where $\overline{D}o$ is the observed mean distance between each feature and its nearest neighbor and is given by

$$\overline{D}o = \frac{\sum_{i=1}^{n} d_i}{n} \tag{3}$$

Table 1 Number of considered rain gauges and the average data record length (years) in each province

Province name	Province code	Number of rain gauges with minimum 30 years record	Average data record length (years)
Riyadh	1	35	44
Makkah Almukaramah	2	37	42
Almadinah Almunawarah	3	25	41
Qassim	4	17	39
Eastern Province	5	11	42
Asir	6	52	43
Tabuk	7	9	44
Hail	8	14	43
Northern boundaries	9	4	44
Jazan	10	21	45
Najran	11	4	41
Albaha	12	12	45
Jouf	13	14	42
Total		255	

and $\overline{D}_E$ is the expected mean distance for the features given in a random pattern and is given by

$$\overline{D}_E = \frac{0.5}{\sqrt{n/A}} \tag{4}$$

In the above Eqs. 2 and 3, d_i equals the distance between rain gauge i and its nearest neighboring rain gauge, n corresponds to the total number of rain gauges (in our case, the number of rain gauges=255), and A is the area of minimum enclosing rectangle around all rain gauges (http://resources.arcgis.com/en/help/ 2015).

The average neighbor z-score for the statistic is calculated as

$$z = \frac{\overline{D}o - \overline{D}_E}{SE} \tag{5}$$

where

$$SE = \frac{0.26136}{\sqrt{n^2/A}} \tag{6}$$

There are three spatial distribution types, namely dispersed, random, and clustered (see Fig. 2). The random type is

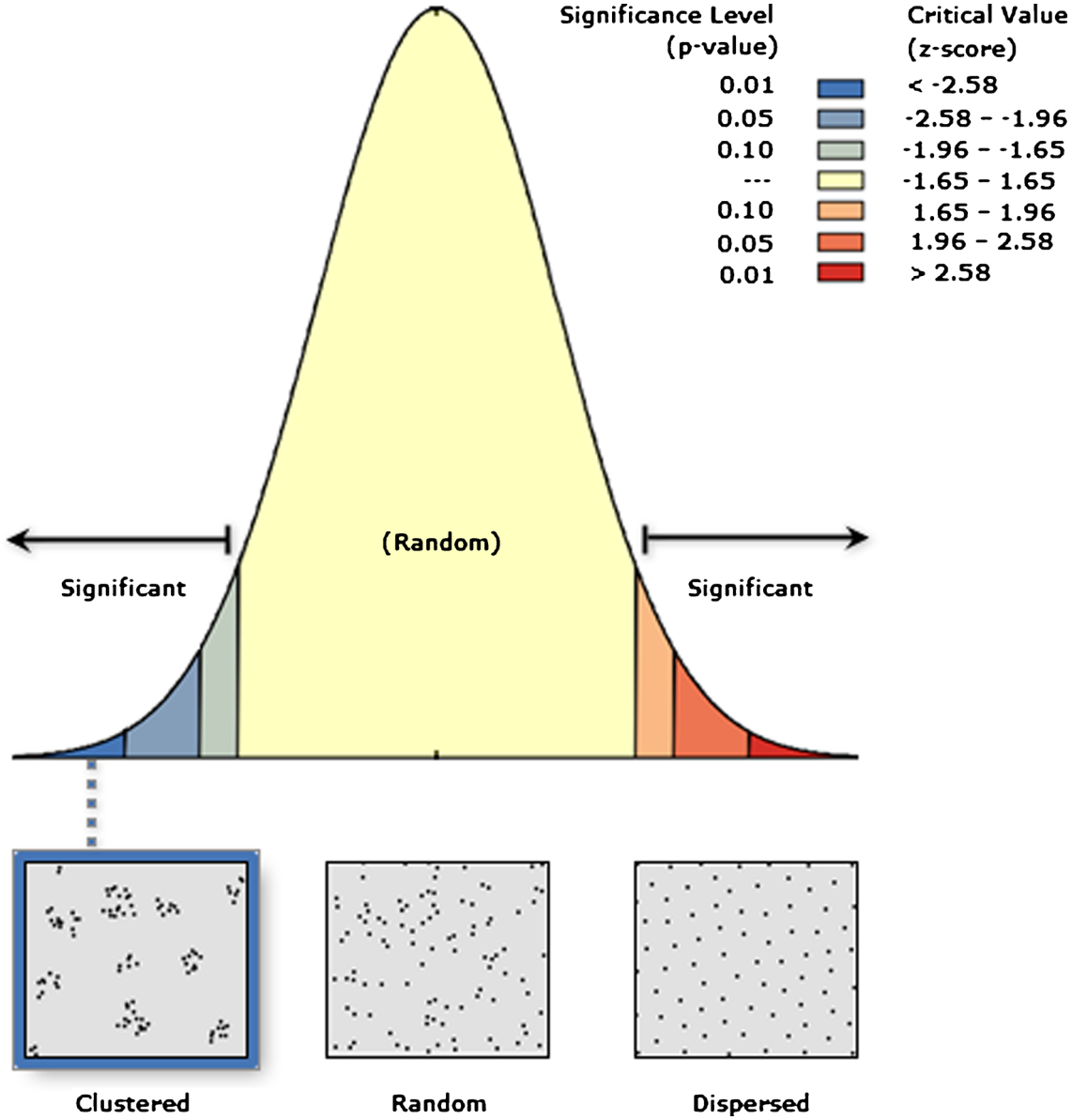

Fig. 2 Rain gauge pattern analysis using average nearest neighbor method

Table 2 Results of average nearest neighbor tool

Observed mean distance	31,518.000041 m
Expected mean distance	43,690.839571 m
Nearest neighbor ratio	0.721387
z-score	−8.511429
p-value	0.000000

characterized by z-score ranging from −1.65 to 1.65, the clustered type has z-score of less than −2.58, and the dispersed has z-score of greater than 2.58. Based on the calculated z-score of approximately −8.5, the spatial distribution of the rain gauge locations is considered to be of the type "clustered." This can clearly be seen by looking at Fig. 1, where the rain gauges are concentrated in the southwest region and the central Riyadh region. Table 2 lists the calculated statistical parameters of the ANN tool.

To obtain the radius of influence of each rain gauge, Thiessen polygons were established around each gauge, and then the polygon area was converted to the equivalent circle (see Fig. 3). The minimum radius of the equivalent circle was found to be 9 km; hence, the grid cell size was considered 8×8 km. This avoids having more than one gauge within any pixel. Chen and Liu (2012) reported that the prediction accuracy increases with increasing the number of known rainfall stations. Therefore, a search radius of 180 km, which is three times the average radius of all equivalent circles, was considered adequate in our case while interpolating the rain data using the different methods. Table 3 lists the parameters used in the different interpolation methods.

Figure 4 shows the spatial distribution of the semivariogram function, γ, previously defined by Eq. 1, for the April rain data. It is clearly seen that within the distance, h, of the selected search radius of 180 km, only the southwest region has γ-values larger than 570 mm^2. This value corresponds to a variation in rainfall depths of approximately 34 mm that is probably due to the heavy rainfall characterizing that region and its complex mountainous topography. Elsewhere,

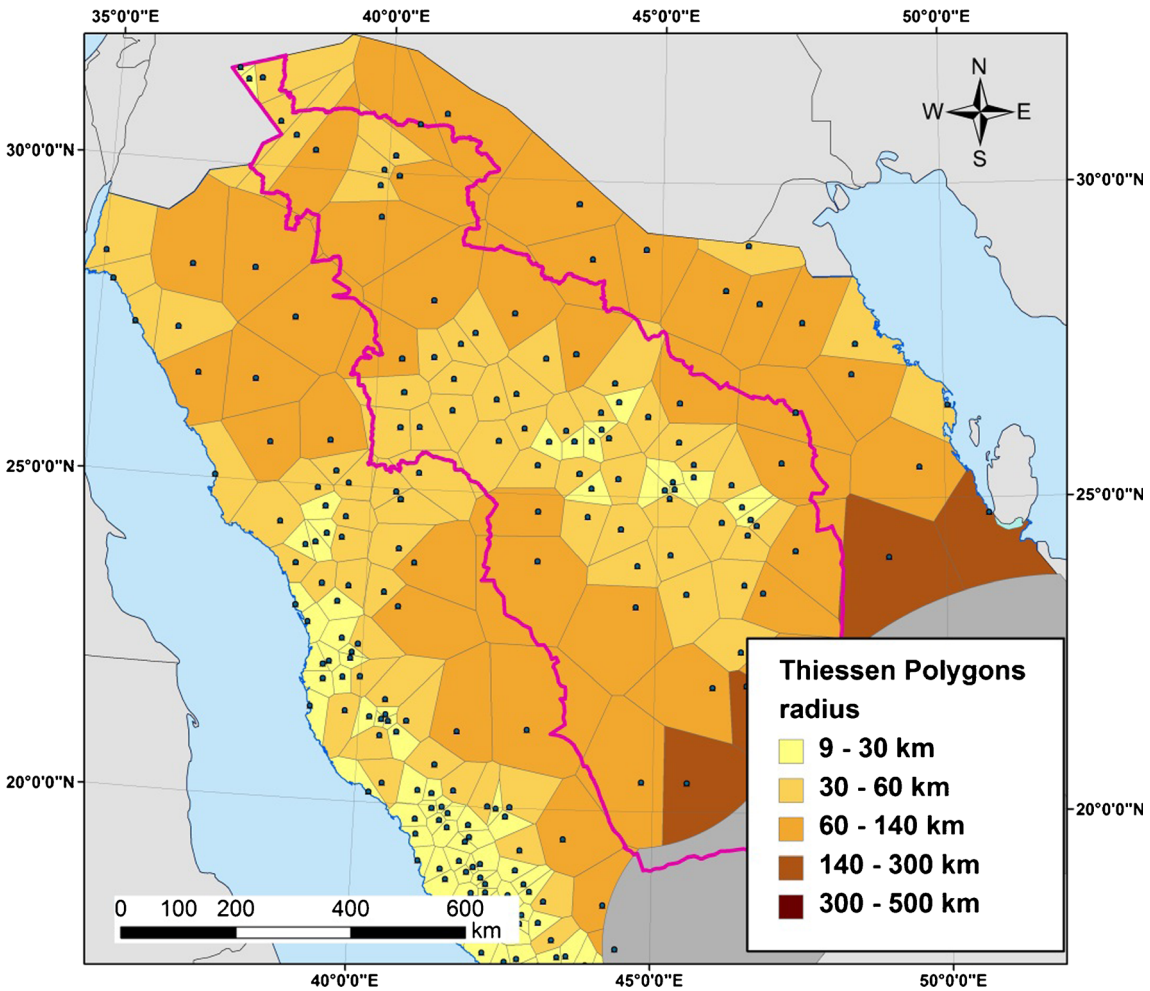

Fig. 3 Rain gauge pattern analysis using Thiessen polygon method

Table 3 Parameters used in the six methods

IDW	Cell size	8000 m
	Power	2
	Search radius (Fixed)	180,000 m
Kriging	Cell size	8000 m
	Kriging method	Ordinary
	Semivariogram models	Spherical
	Search radius (Fixed)	180,000 m
Spline	Cell size	8000 m
	Spline type	Regularized
	Weight	0.1 (default)
	Number of points	12 (default)
Natural neighbor	Cell size	8000 m
Modified Shepard method	Smoothing factor	0
	Quadratic neighbors	13
	Weighting neighbors	19
TIN	Cell size	8000 m

however, the γ-values are much smaller, which indicates less variability in rainfall.

Results and discussion

Detection of the locations receiving maximum precipitation

In order to detect the locations receiving maximum precipitation, the percentage of mean monthly precipitation to the total mean annual precipitation for all months was calculated and is shown in Fig. 5. It can be seen from Fig. 5 that the highest monthly precipitation percentages in KSA occur during the months of November to April, i.e., a period of 6 months.Therefore, analyses of rainfall data for these months were done to select the locations having maximum rainfall.

Determining the optimal method of interpolation for developing isohyetal maps

Rainfall measurements are commonly observed at point locations, i.e., rain gauges. Due to the relatively far distances between the rain gauges and engineering projects that may be located in areas that have no gauges, these measurements are required to be converted to grid raster format using interpolation methods. There are several methods used to generate isohyetal maps; for example, Mair and Fares (2011) used Thiessen polygon, inverse distance weighting (IDW), linear regression, ordinary kriging, and simple kriging with varying local means to estimate wet and dry season rainfall. Belani and Alhassoun (2012) compared between different interpolation methods in estimating missing rain data. In the following sections, brief description of the six methods used in this study will be given. Spatial analyst tools of ArcGIS 10.0 and SURFER 7.0 were used to compare between these six interpolation methods as will be shown later.

Figure 6 shows the resulting isohyetal maps developed adopting the abovementioned six interpolation methods using spatial analyst tools in ArcGIS 10.0 and SURFER 7.0. The controlling parameters used in each of these methods are listed in Table 3. From Fig. 6, it can be seen that each method resulted in different spatial distribution of the rain data.

The isohyetal map that resulted from kriging method, for example, shows overall gradual variation of the rainfall. Kriging method is typically known as "BLUE," which stands for best linear unbiased estimator. This has the consequence of not allowing detecting areas of maximum rainfall within the region. The isohyetal map that resulted from spline method, on the other hand, reflects relatively abrupt changes, known as

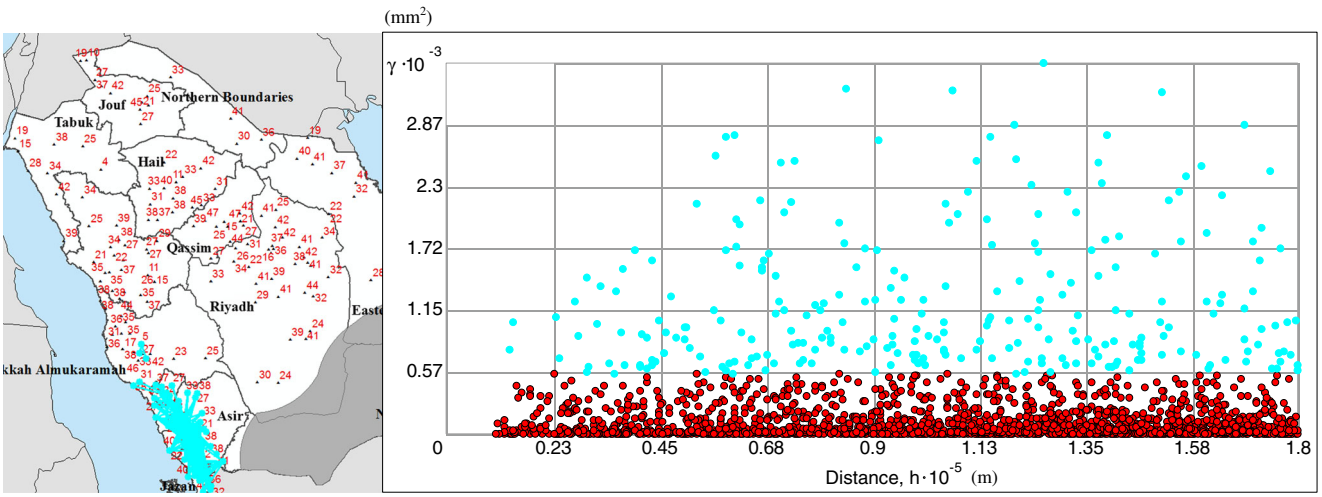

Fig. 4 The spatial distribution of the semivariogram function, γ (the reflection of the values is shown to the left on the map of KSA)

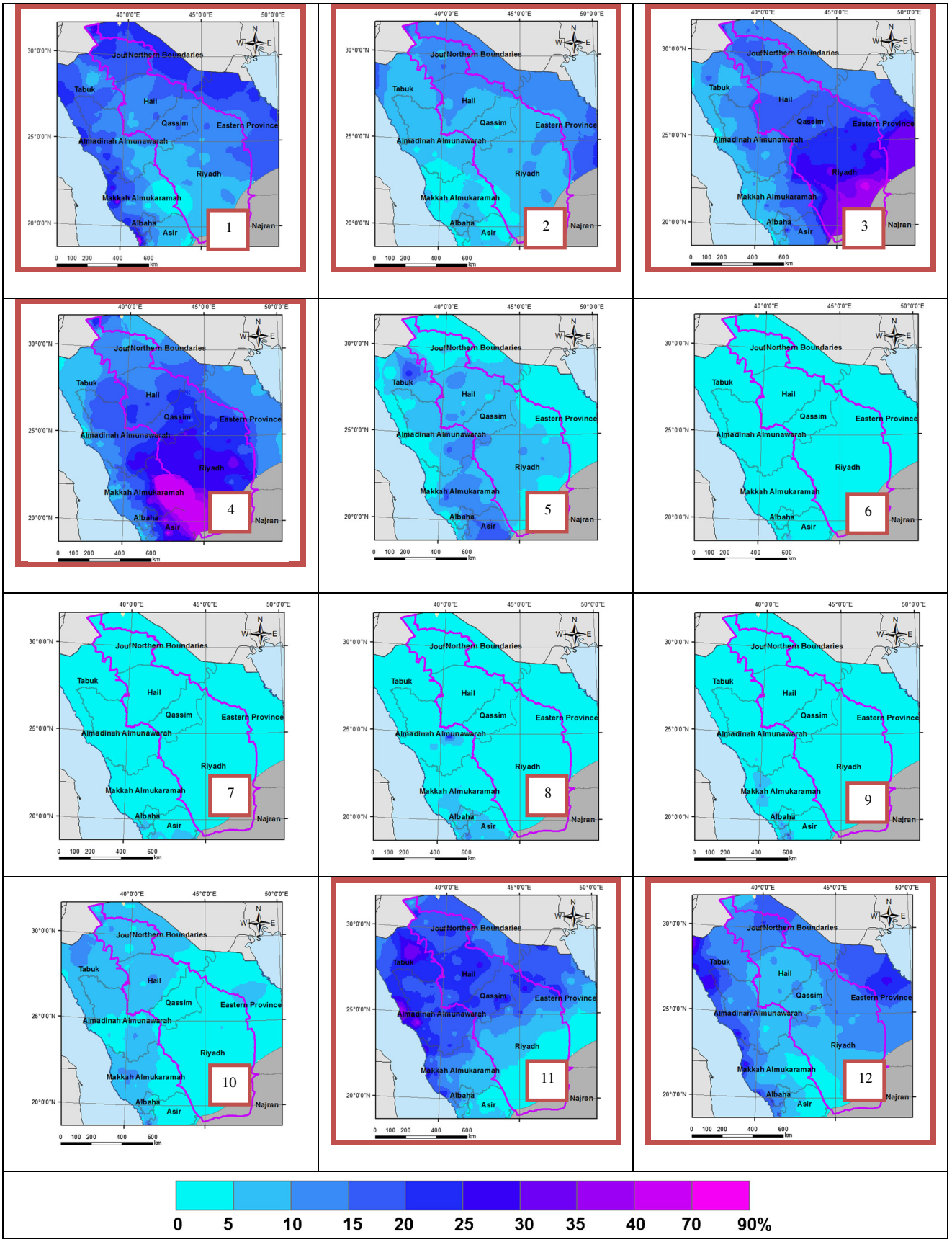

Fig. 5 Isoheytal maps showing the ratio of mean monthly precipitation to the total mean annual precipitation for all months (1=Jan. …. 12=Dec.)

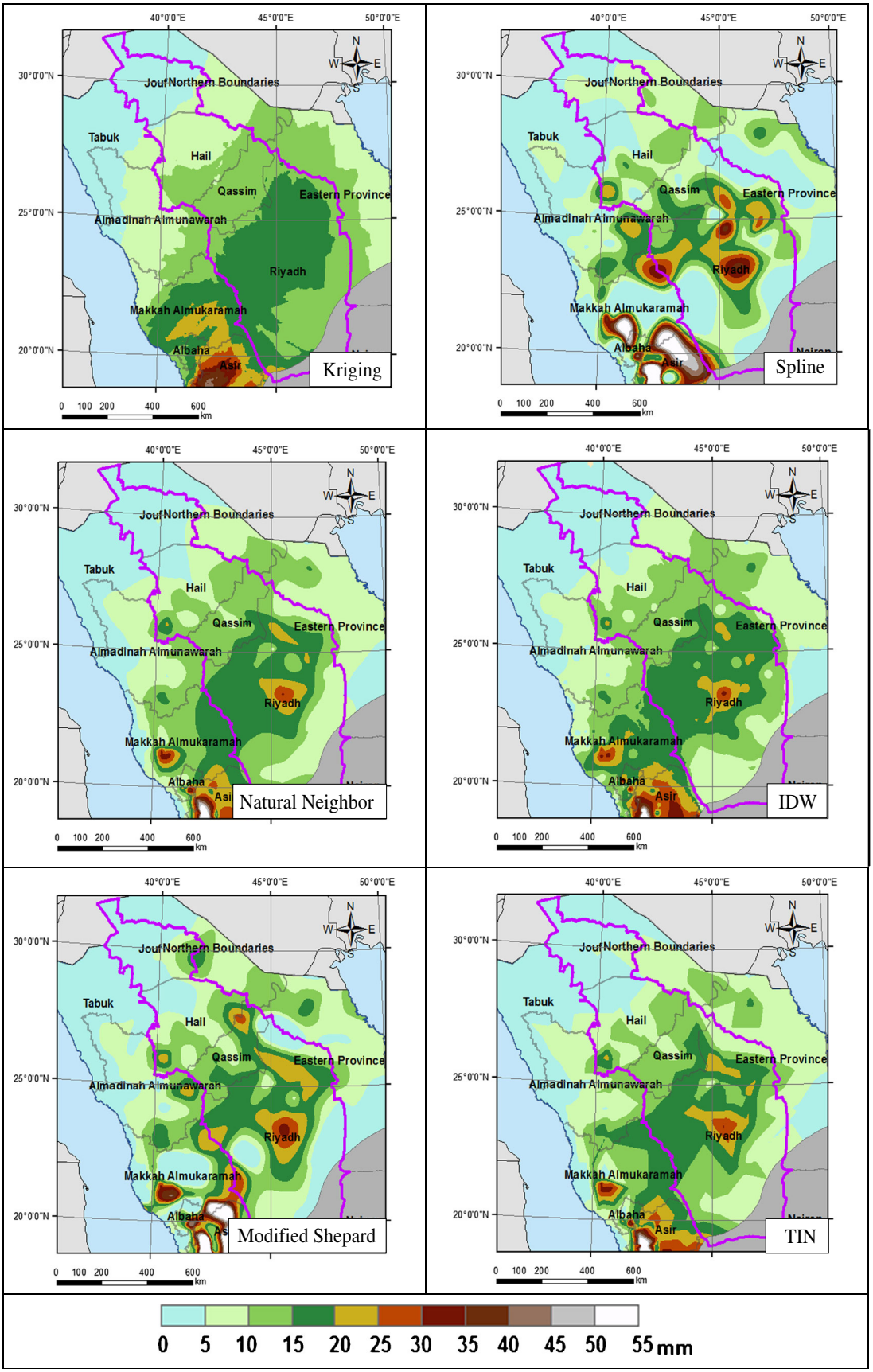

Fig. 6 Isohyetal maps developed by the six interpolation methods: kriging, spline, natural neighbor, IDW, modified Shepard, and TIN

bull's eye, in the spatial rainfall distribution. This is due to this method depending mainly on the data at the gauge locations and not considering the surrounding areas with no gauges. Both the IDW and natural neighbor methods resulted in isohyetal maps that generally show gradation in the spatial rainfall distribution, notwithstanding reflecting the local effects of the rain gauge data. While the modified Shepard's method was developed to get rid of the bull's eye effect, it can be seen that this problem is quite obvious as shown in Fig. 6. Because the rain gauges are not evenly distributed over the grid area, distinct triangular facets appear on the map as Yang et al. (2004) mention (see Fig. 6). Because the bull's eye effect is obvious in the resulting maps of quite few methods of the six presented in Fig. 6, it is required to assess the accuracy of each method quantitatively.

Assessing the accuracy of interpolation methods

The accuracy of the adopted interpolation methods was assessed by estimating rainfall at the rain gauges using the grid raster generated by each interpolation method and then calculating the residual between the estimated and observed data. The rainfall data of April, as an example month within the period of highest monthly precipitation percentage of the total mean annual precipitation (review Fig. 5), was used for this purpose. Table 4 lists the statistical parameters of the residuals for each method. From the results in Table 4, it can be seen that the IDW has the minimum standard deviation. Also, the minimum absolute value of the residuals is of IDW, whereas the smallest absolute average value of the residuals is that of spline method. While the results listed in Table 4 indicate that both IDW and modified Shepard have fairly close standard deviation and minimum residual, yet, the modified Shepard has much larger maximum residual as compared to IDW. The percentage of residuals within ±2.0 mm were also calculated and found to be 98 % for IDW, modified Shepard and TIN, 97 % for natural neighbor, 90 % for spline, and 32 % for kriging. It is to be noted here that Dirksa et al. (1998) also reported that IDW provided the best results in their study, in addition to its shorter processing time. Therefore, IDW was selected to be used for developing the monthly isohyetal maps as will be shown later.

Studying the months of higher rainfall in the central zone of KSA

As shown earlier in Fig. 5, the highest percentage monthly precipitation of the total annual precipitation was found to occur during the 6 months: November–April. In this section, the IDW interpolation method will be used to develop the grid raster, which represents isohyets based on available measurements of rainfall at the rain gauges, for these months. Figure 7 shows the resulting isohyetal maps for these 6 months: November–April. From Fig. 7, it is seen that during January, the higher precipitation occurs within the eastern and western regions of KSA; moderate precipitation is also observed east of Riyadh and Qassim. During February, an obvious decrease in precipitation is observed throughout most of KSA, except for some regions on the Gulf Coast in the Eastern Province. In March, the highest precipitation occurs northeast of Riyadh, whereas in April, it moves to south central Riyadh. During November, the precipitation becomes less in Riyadh but increases in Qassim and Hail. In December, the highest precipitation occurs in the eastern and western provinces, while it decreases in Riyadh.

Statistical analyses of the grid raster

In the Zonal Statistics tools in ArcToolbox, ArcGIS 10.0 was used to analyze the grid raster that was generated using the IDW interpolation method for the provinces of the Central Zone being the study area. Table 5 shows the statistical parameters of the maximum monthly rainfall in these provinces during the 6 months of higher percentage precipitation of the total annual precipitation.

From the results in Table 5, it can be seen that the maximum monthly rainfall occurs during March in Riyadh. Also, the second maximum monthly record is during April with fairly close value to that of March; note that the other statistical parameters are almost equal for both months. Therefore, further investigation for these 2 months for Riyadh Region

Table 4 The statistical parameters of the residuals of the adopted six interpolation methods

Parameter	IDW	Kriging	Natural neighbor	Spline	Modified Shepard	TIN
Minimum (mm)	0.001	0.097	0.008	0.006	0.001	0.009
Maximum (mm)	0.704	10.912	3.601	3.422	2.678	3.928
Average (mm)	−0.085	−0.435	0.08	0.06	0.059	−0.048
Standard deviation (mm)	0.507	4.781	0.838	0.994	0.669	0.768

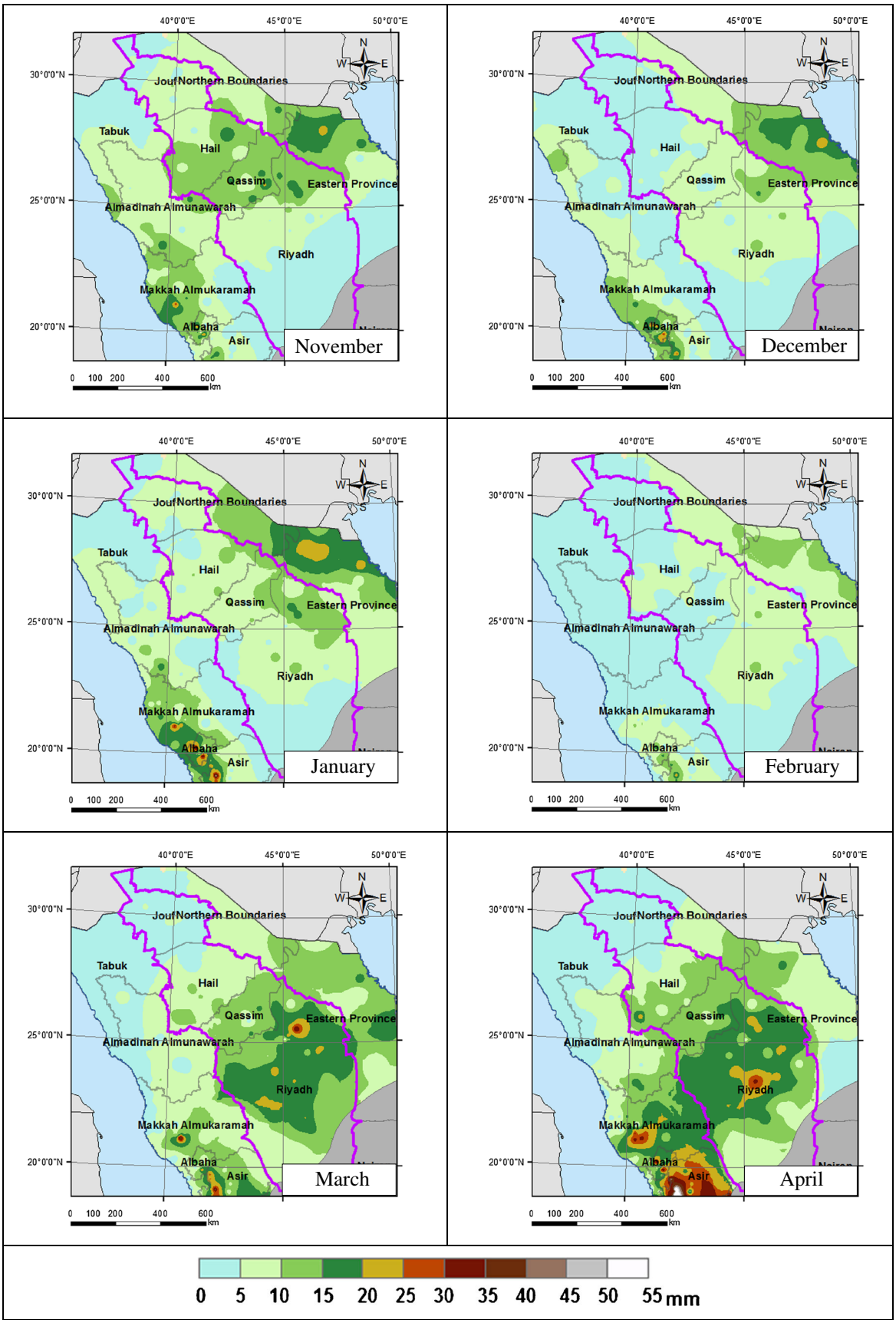

Fig. 7 Isohyetal maps developed using inverse distance weighted (IDW) interpolation during the months of higher percentage precipitation

Table 5 Statistical parameters of the IDW interpolation in the central zone provinces

	Month	Minimum (mm)	Maximum (mm)	Mean (mm)	Standard deviation (mm)
Riyadh	January	0.07	18.1	5.96	3.48
	February	0.67	12.05	4.8	2.27
	March	5.59	34.55	14.25	4.35
	April	5.2	30.94	14.23	4.55
	November	0.07	19.36	4.77	4.2
	December	0.35	16.5	5.49	3.17
Qassim	January	3.33	13.98	8.64	1.82
	February	0.99	8.8	4.73	1.12
	March	2.78	16.21	11.24	1.61
	April	5.39	17.01	12.8	1.66
	November	4.61	22.08	11.9	2.11
	December	2.01	10.08	6.39	1.22
Hail	January	2.21	12.17	7.17	2.01
	February	1.93	9.42	5.09	1.14
	March	2.42	13.89	7.72	2.11
	April	2.35	22.02	8.99	3.03
	November	4.23	18.22	10.39	2.37
	December	0.61	8.04	4.18	1.28
Jouf	January	2.54	9.72	5.47	1.05
	February	1.22	5.77	3.27	0.6
	March	0.97	6.18	4.1	0.81
	April	1.46	5.67	3.36	0.51
	November	0.76	10.62	5.46	1.41
	December	0.41	6.22	3.76	1.01

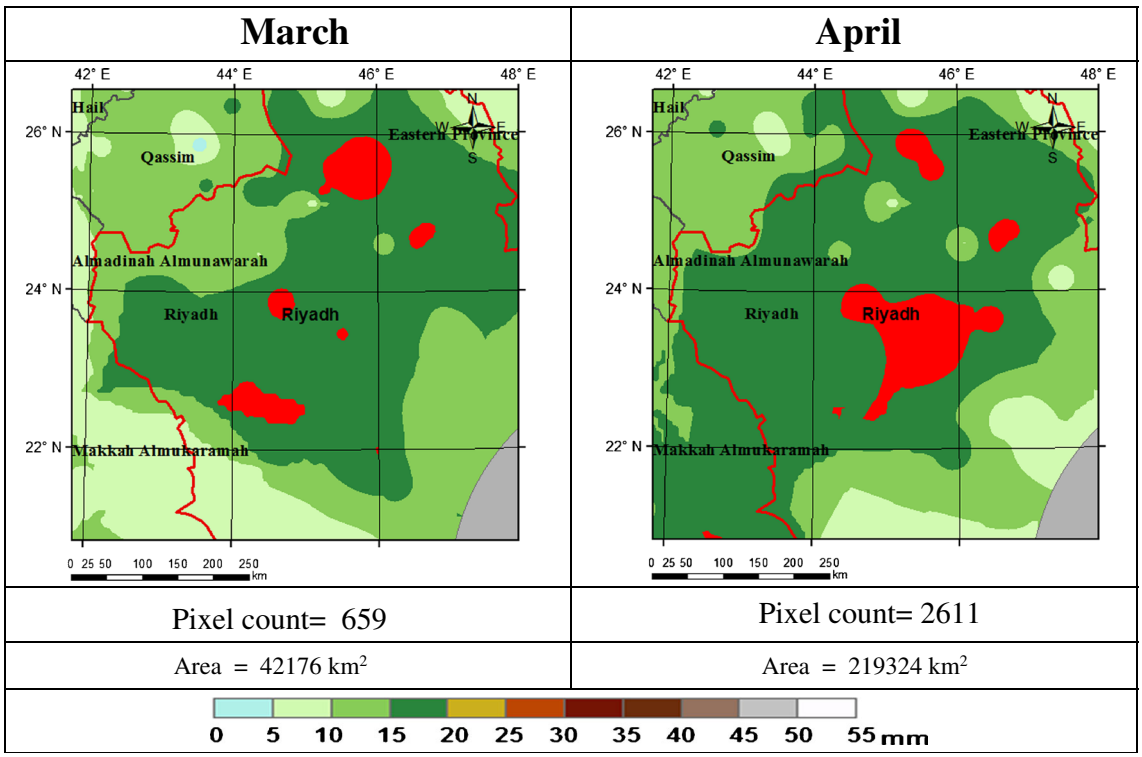

Fig. 8 Comparison of the rainfall spatial distribution during March and April in Riyadh Region

will be carried out in the following section. For Qassim, on the other hand, the maximum monthly rainfall occurs during November, whereas the highest mean monthly rainfall is during April. In Hail, April reflects the maximum monthly rainfall, whereas November has the highest mean monthly rainfall. Alternatively in Jouf, the maximum monthly rainfall and the highest mean monthly rainfall are both during November. It is also noticeable that the values of the standard deviation are highest during the months that have the largest maximum monthly rainfall.

Finding suitable sites for water harvesting

By referring to the results in Table 5, it was shown that both March and April reflected the highest maximum daily and mean monthly rainfall in Riyadh Region. Using the selected

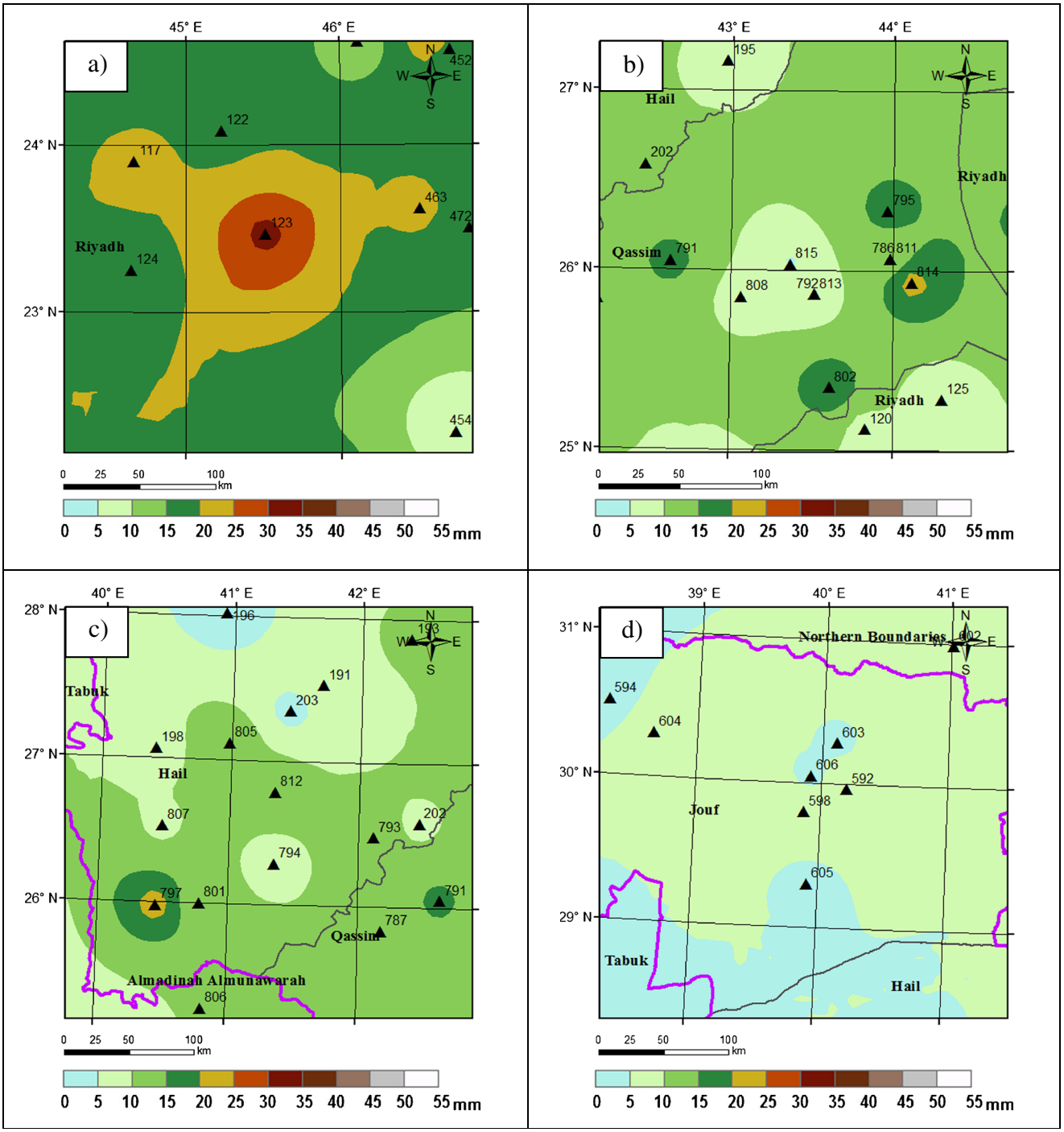

Fig. 9 The isohyetal maps of the maximum monthly rainfall in **a** Riyadh, **b** Qassim, **c** Hail, and **d** Jouf

interpolation method of IDW, the isohyetal maps for March and April data were generated and are presented in Fig. 8. It can be seen from Fig. 8 that the area covered by the higher maximum rainfall of March is actually much smaller than that of April. This results in higher potential for water harvesting during April than March in Riyadh Region. A simple comparison of the pixel counts (1 pixel=8×8 km^2) for the areas with rainfall of 20 mm and larger is shown in Fig. 8. It is seen than in April, an area of approximately 219.3 km^2 will likely receive 20 mm or larger rainfall, as opposed to an area of only approximately 42.2 km^2 in March.

Figure 9 shows the spatial distribution of the maximum monthly rainfall during the months of its highest values as listed in Table 5, except for Riyadh Region (Fig. 9a) where the isohyetal map is of April based on the area coverage comparison presented previously in Fig. 8. The locations of the rain gauges, and the longitudes and latitudes are also shown; for example, in Riyadh Region, the area of the highest maximum monthly rainfall is around gauge no. 123 (Al-Rain Station). Potential water harvesting sites may be selected within the area bounded by 23 to 24 N, and 45 to 46 E. In Qassim (Fig. 9b), the areas of the highest maximum monthly rainfall during November are distributed around gauges 791, 795, 802, and 814; note that the highest mean monthly rainfall occurred at gauge 814. The area bounded by 25.5 to 26.5 N, and 43.5 to 44.5 E may present potential water harvesting sites in Qassim. Figure 9c shows the isohyetal map for Hail during April; the areas of the highest maximum monthly rainfall are near the western boundary of Hail neighboring Almadinah Almunawarah; the highest maximum monthly rainfall occurred at Gauge 797. The area bounded by 26 to 27 N, and 40 to 43 E shows higher potential for water harvesting sites. Figure 9d shows the isohyetal map for Jouf during November. It is seen that the Jouf Province overall receives little rain (less than 10 mm); this may be indicative that the province may not have high potential for water harvesting. Note that the highest maximum monthly rainfall occurred at gauge 598 (Domet Al-jandal Station).

Conclusions and recommendations

- This article presents the results of studying the spatial distribution of monthly rainfall based on data of 255 rain gauges with records of longer than 30 years that are scattered across the Kingdom of Saudi Arabia (KSA).
- Analyses of the spatial distribution of the rain gauge locations across KSA, based on the Average Nearest Neighbor function, showed that they are of the type clustered.
- Investigation of the semivariogram function for all rain gauges across KSA indicated that only the southwest mountainous region has high rainfall depth variability; otherwise, the other regions, especially the central zone under study, have much less rainfall variability.
- The study also includes comparison of the results of six different interpolation methods that were used for the spatial rainfall distribution using GIS to detect suitable regions for water harvesting within provinces of the central zone of KSA, namely Riyadh, Qassim, Hail, and Jouf. The interpolation methods are kriging, spline, natural neighbor, inverse distance weighting (IDW), modified Shepard, and triangulation with linear interpolation (TIN).
- Based on statistical parameters of the residuals at the rain gauges, the IDW method of interpolation proved most successful when compared to the other five methods, for generating the isohyetal maps. The results of the modified Shepard method were the second closest to IDW's. The percentage of residuals within ±2.0 mm were also calculated and found to be 98 % for IDW, modified Shepard and TIN, 97 % for natural neighbor, 90 % for spline, and 32 % for kriging.
- The detection of the water harvesting regions included in this study is based on only rainfall as the most important parameter for water harvesting. It is recommended, however, to expand on this study by including other parameters, such as the geomorphology and topography of individual watersheds/sites, nearness of sites to communities, and their accessibility. This will require delineating water harvesting sites within the regions recommended herein.

Acknowledgments The authors would like to thank the Chair of Prince Sultan Bin Abdulaziz International Prize for Water of Prince Sultan Institute for Environmental, Water and Desert Research at King Saud University for the provided financial and technical support. The authors thank, as well, Dr. Abdulaziz S. Al-Turbak, hydrology professor of the Civil Engineering Department at King Saud Univesrity, Dr. Rabie S. Fouli, former World Meteorological Organization (WMO) Expert, and Mr Oumar Lafoza of King Abdulaziz City for Science and Technology (KACST) for their revision of the manuscript and the productive discussions of the topic.

References

Abouammoh AM (1991) The distribution of monthly rainfall intensity at some sites in Saudi Arabia. Environ Monit Assess 17:89–100

Al-Adamat R (2008) GIS as a decision support system for siting water harvesting ponds in the Basalt Aquifer/NE Jordan. J Environ Assessment Policy Manag 10(2):189–206

Al-Adamat R, Diabat A, Shatnawi G (2010) Combining GIS with multicriteria decision making for siting water harvesting ponds in Northern Jordan. J Arid Environ 74(11):1471–1477

Alazba AA (2004) Contour maps for hydrologic and climatic parameters in Saudi arabia, American Society of Agricultural and Biological Engineers, Paper number 042096. ASAE Annual Meeting. doi: 10.13031/2013.16379

AlHassoun SA (2011) Developing an empirical formulae to estimate rainfall intensity in Riyadh region. J King Saud Univ Eng Sci 23: 81–88

Al-Turbak AS, Quraishi AA (1986) Regional flood frequency analysis for some selected basins in Saudi Arabia. Proceedings of International Symposium on Flood Frequency and Risk Analysis, Louisiana State University, Baton Rouge, La., Volume on Regional Flood Frequency Analysis, pp. 27–34

Al-Zahrani MAM (1989) Status of hydrological network in south-western region of the Kingdom of Saudi Arabia. M.Sc. Thesis at Faculty of the College of Graduate Studies of King Fahd University of Petroleum & Minerals, Dhahran, Saudi Arabia

Al-Zahrani MAM, Hussain T (1998) An algorithm for designing a precipitation network in the south-western region of Saudi Arabia. J Hydrol 205:205–216

Amin MT, Alazba AA, Manzoor U (2013) Soft path water management in dry and arid regions of the Arabian Peninsula by rainwater harvesting. Am J Environ Sci 9(2):156–163. doi:10.3844/ajessp.2013.156.163

ArcGis Resources Website (2015) (http://resources.arcgis.com/en/help/); Accessed on 19 Jan. 2015

Bakir M, Xingnan Z (2008) GIS and Remote Sensing Applications for Rainwater Harvesting in the Syrian Desert (Al-Badia). In Proceedings of Twelfth International Water Technology Conference, IWTC12. Alexandria, Egypt, pp 73–82

Bargaoui ZK, Chebbi A (2009) Comparison of two kriging interpolation methods applied to spatiotemporal rainfall. J Hydrol 365:56–73

Belani HM, Alhassoun SA (2012) Derivation of digital rainfall model to estimate missing rainfall data in Riyadh region. J King Saud Univ Eng Sci 24(2):72

Chen FW, Liu CWL (2012) Estimation of the spatial rainfall distribution using inverse distance weighting (IDW) in the middle of Taiwan. Paddy Water Environ 10(3):209–222

Climate Atlas of Saudi Arabia (1988) Publication of ministry of agriculture and water (now Ministry of Water and Electricity) in cooperation with the Saudi Arabian-United States joint commission on economic cooperation

de Winnaar G, Jewitt GPW, Horan M (2007) A GIS-based approach for identifying potential runoff harvesting sites in the Thukela River basin, South Africa. Phys Chem Earth Parts ABC 32:15–18, 1058–1067

Dirksa KN, Hayb JE, Stowa CD, Harrisa D (1998) High-resolution studies of rainfall on Norfolk Island: Part II: interpolation of rainfall data. J Hydrol 208:187–193

Elsebaie IH (2011) Rainfall intensity-duration-frequency relationship for some regions in Saudi Arabia. Int J Sustain Water Environ Syst 2(1): 7–16

Franke R, Nielson G (1980) Smooth interpolation of large sets of scattered data [J]. Int J Numer Methods Eng 15(2):1691

Gould J, Nissen-Petersen E (1999) Rainwater catchment systems for domestic supply: design, construction and implementation. IT Publications, London

Hadadin N, Shawash S, Tarawneh Z, Banihani Q, Hamdi MR (2012) Spatial hydrological analysis for water harvesting potential using ArcGIS model: the case of the north-eastern desert, Jordan. Water Policy 14:524–538

Lynch SD converting point estimates of daily rainfall onto a rectangular grid. http://proceedings.esri.com/library/userconf/proc98/proceed/to200/pap196/p196.htm. Accessed 23 October 2014

Mahmoud SH, Alazba AA (2014) The potential of in situ rainwater harvesting in arid regions: developing a methodology to identify suitable areas using GIS-based decision support system. Arab J Geosci. doi:10.1007/s12517-014-1535-3

Mahmoud SH, Alazba AA, Amin MT (2014) Identification of potential sites for groundwater recharge using a GIS-based decision support system in Jazan Region-Saudi Arabia. Water Resour Manag 28: 3319–3340. doi:10.1007/s11269-014-0681-4

Mair A, Fares A (2011) Comparison of rainfall interpolation methods in a mountainous region of a tropical island. J Hydrol Eng

Renka RJ (1988) Quadratic Shepard method for bivariate interpolation of scattered data. ACM Trans Math Softw 14(2):149–150

Sibson R, Interpolating Multivariate Data (1981) A brief description of natural neighbor interpolation. Wiley, New York, pp 21–36

Subyani AM (2011) Hydrologic behavior and flood probability for selected arid basins in Makkah area, western Saudi Arabia. Arab J Geosci 4:817–824. doi:10.1007/s12517-009-0098-1

Wheater HS, Butler AP, Stewart EJ, Hamilton GS (1991a) A multivariate spatial-temporal model of rainfall in southwest Saudi Arabia. I. Spatial rainfall characteristics and model formulation. J Hydrol 125:175–199

Wheater HS, Onof C, Butler AP, Hamilton GS (1991b) A multivariate spatial-temporal model of rainfall in southwest Saudi Arabia. II. Regional analysis and long-term performance. J Hydrol 125:201–220

WMO (1989) Calculation of monthly and annual 30-years standard normals. WCDP, No. 10, WMO-TD/No. 341, Geneva

Yang C, Kao S, Lee F (2004) Twelve different interpolation methods: a case study of surfer 8.0, international congress for photogrammetry and remote sensing, pp 778–785